Analysis of Orbital Perturbational Effects on Earthbound Spacecraft

Kevin Iverson, Mike Kabot

California Polytechnic State University, San Luis Obispo

December 8, 2023

Dr. Kira Abercromby

AERO 452 - Spaceflight Dynamics II

I. INTRODUCTION

In the analysis of the effects perturbations have on orbital objects, an important factor to consider is the orbital regime that the objects reside in. Effects can vary drastically within LEO based on local atmospheric density (a function of altitude), and beyond LEO where drag is no longer the dominant perturbation, effects like solar radiation pressure and n-body effects can have more impact on the orbital elements of objects. The following objects were selected for analysis of perturbations in different orbit regimes:

- **LEO Object:** International Space Station (ISS)

As an object in LEO with extremely high area and mass, the ISS was determined to be an interesting case study for the effects of perturbations present in LEO. The ISS was initialized with the following two-line element set (TLE):

```
1 25544U 98067A   23339.58703728  .00015059  00000+0  26943-3 0  9996
2 25544  51.6407 199.5862 0001156  12.7831  76.8411 15.50199867428372
```

After converting the TLE into classical orbital elements, a MATLAB function was used to compute the initial state vectors, which were propagated to visualize the osculating orbit. The results are show below:

Figure 1: ECI Plot of ISS osculating orbit

The ISS has the following physical parameters, which will later be utilized in calculating perturbing accelerations:

C_d	2.2
A (m^2)	1000
m (kg)	430000

- **Non-LEO Object (GEO):** Astranis Arcturus

In order to examine the effects of objects outside the influence of atmospheric drag, an object with sufficiently high altitude was selected. Arcturus, which is a micro-GEO internet satellite, was selected. Arcturus was initialized with the following two-line element set (TLE):

```
1 56371U 23060B   23290.62836976  .00000142  00000-0  00000-0 0  9993
2 56371   0.2510  88.6318 0002573 167.6611 192.8044  1.00270258  1690
```

After converting the TLE into classical orbital elements, a MATLAB function was used to compute the initial state vectors, which were propagated to visualize the osculating orbit. The results are show below:

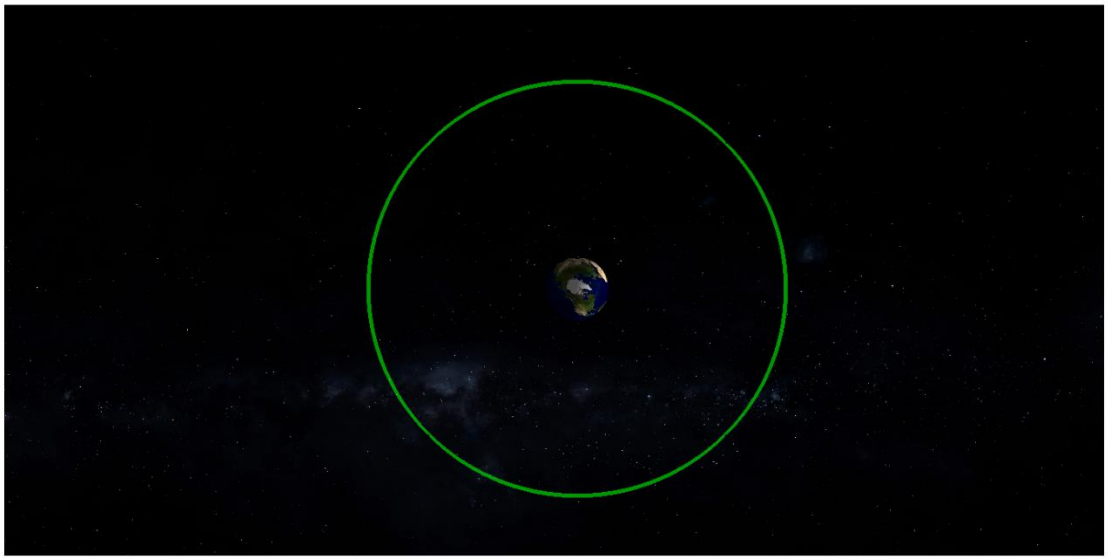

Figure 2: ECI Plot of Arcturus osculating orbit

Arcturus has the following physical parameters, which will later be utilized in calculating perturbing accelerations:

C_d	2.2
A (m^2)	20
m (kg)	300

- **Specialty Orbit Object:** Landsat 9

An additional part of the analysis involved the examination of a spacecraft that took advantage of orbital perturbations to perform some specialty function – examples of these orbits include Sun Synchronous Orbit (SSO), Molniya orbits, and orbits taking advantage of Earth-Moon Lagrange points. Landsat 9, a spacecraft operating in SSO, was selected with the intent of analyzing how it takes advantage of non-spherical gravitational perturbations. Landsat 9 was initialized with the following two-line element set (TLE):

```
1 49260U 21088A   23341.20999672  .00000490  00000-0  11874-3 0  9994
2 49260  98.2126  48.8670 0001172  94.4972 265.6360 14.57128335116599
```

After converting the TLE into classical orbital elements, a MATLAB function was used to compute the initial state vectors, which were propagated to visualize the osculating orbit. The results are show below:

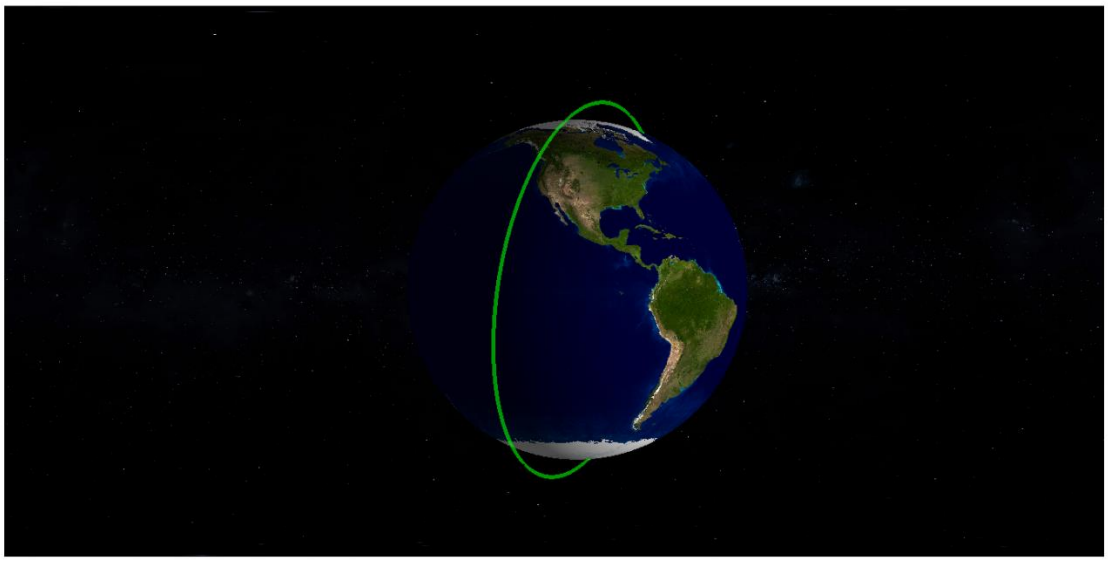

Figure 3: ECI Plot of Landsat 9 osculating orbit

Landsat 9 has the following physical parameters, which will later be utilized in calculating perturbing accelerations:

C_d	2.2
A (m^2)	21.8
m (kg)	2711

II. METHODOLOGY

All parts of the project utilized Cowell's Method to propagate all orbital trajectories. Cowell's Method operates by taking an initial state of the object and propagating the trajectory forward by integrating the equations of motion with respect to time. As the project was done in MATLAB, Cowell's Method was used in conjunction with the ode45 solver with a variable time step to integrate all equations of motion. Cowell's Method was chosen over other propagation methods such as the Variation of Parameters method and Encke's Method due to its ease of use and lack of timestep related errors found in the other methods. Encke's method was first attempted but ran into errors when attempting to include the J2 perturbation.

A standard two body approximation of orbital motion is first completed, only accounting for the gravitational force of the Earth, yielding the following equations of motion:

$$\ddot{\boldsymbol{x}} = -\frac{\boldsymbol{\mu}}{\boldsymbol{r^3}}\boldsymbol{x}$$

$$\ddot{\boldsymbol{y}} = -\frac{\boldsymbol{\mu}}{\boldsymbol{r^3}}\boldsymbol{y}$$

$$\ddot{\boldsymbol{z}} = -\frac{\boldsymbol{\mu}}{\boldsymbol{r^3}}\boldsymbol{z}$$

Where μ is the gravitational parameter of Earth, assumed to be 398600 $\frac{km^3}{s^2}$ and r is the position vector of the spacecraft in ECI coordinates. All osculating orbits plotted in this report were propagated using Cowell's Method with these equations of motion. In order to propagate the trajectories with orbital perturbations included the acceleration due to each of the perturbations was added to these equations. The perturbations included for this analysis were aerodynamic drag, non-spherical Earth, n-body, and solar radiation pressure.

For aerodynamic drag, an exponential model of density was used for Earth's atmosphere up to 1000 km. At each step of the integration, the altitude was calculated from the inputted position vector radius and was sent to an exponential density function which returned a value for the density of the atmosphere at that point. In conjunction with the drag coefficient Cd, mass m, and relative velocity of the spacecraft to the Earth V_{rel}, the acceleration due to drag can be calculated by

$$a_{drag} = -\frac{C_d A}{2m} * \rho * ||V_{rel}|| * V_{rel}/||V_{rel}||$$

For this project, aerodynamic drag was only considered for objects operating Low Earth Orbit (LEO) regime and was not included for any object in GEO or further.

For the non-sphericity of Earth, only the J2-J6 zonal harmonics were considered, with no inclusion of the tesseral harmonics given the scope of this project. The perturbational acceleration components for the J2-J6 perturbations were summed and added to the overall acceleration of eh spacecraft. Due to the length and complexity of these equations, they are not listed below.

For the n-body perturbation, the position of the spacecraft relative to the Sun in ECI coordinates, R_s, is first found. This is done by first finding the position of the Sun in ECI at a specified Julian date, then subtracting the position vector, R, of the spacecraft. Along with the gravitational parameter of the Sun, μ_{sun} , equal to 132.7e9 $\frac{km^3}{s^2}$, the n-body acceleration can be found from

$$a_{nbody} = \frac{\mu_{sun}}{||R_{rel}||^3} * F * R_s - R$$

It is important to note that for the purpose of this project, only the Sun was considered as an extra body in the Sun-spacecraft system.

To find the acceleration due to solar radiation pressure, the same relative position to the Sun, R_s, was found, in conjunction with a function F where F describes whether the spacecraft is in sunlight or shadow, with F = 0 in shadow and F = 1 in sunlight. In conjunction with the assumptions that the reflectivity, C_r, constant of all spacecraft was 1.2 and that the solar radiation pressure, P_{srf}, was constant and equal to 4.57e-6 Pa, the acceleration was found by

$$a_{SRP} = -P_{srf} * C_r * \frac{A}{m} * \frac{R_s}{||R_s||} * F$$

Where A and m are again the respective spacecraft frontal area and mass.

For Part 1, both objects were propagated forward 100 days with these perturbational accelerations added to the two body equations of motion stated earlier. In Part 3, the Landsat 9 satellite was propagated forward 365 days to show its full coverage and nodal progression.

As part of the analysis for Part 1, it was necessary to compute the Delta-V required to correct the perturbations. In order to compute a transfer trajectory between the osculating and perturbed orbits, a Lambert's solver was implemented between a point on the perturbed orbit and a final point on the osculating orbit some undetermined timestep later. Given that the total Delta-V would change as a function of both transfer time and positional differences of the two orbits, the final Delta-V was found using an optimization method. To simplify the problem some and make propagating orbits using Cowell's method quicker, a "drift" time of 1 day was arbitrarily assigned before correcting the perturbed trajectory. An iterative loop was then used to find the total Delta-V required for three transfers at varying transfer times, ranging from 5 minutes to 35 minutes, which was plotted to determine the minimum (Figure 9). After this was complete, the final permutation with the lowest Delta-V requirement was used for the trajectory correction.

To correct the perturbed orbit, the same Lambert's problem used in the optimization step was again used, this time with the previously defined drift time and the newly obtained transfer time. Cowell's method was used to propagate the initial perturbed orbit for the drift time, in addition to propagating the osculating orbit to the *final* time (drift time plus transfer time). The last elements of these solution arrays were then used as inputs to the Lambert's solver, which computed the intermediate trajectory, as well as the total Delta-V for the maneuver. This process was repeated for three correction maneuvers, which are plotted in Figure 10, and further details are discussed below.

III. RESULTS AND DISCUSSION

a. LEO Object Analysis

First, the International Space Station was propagated forward 100 days with all perturbations included, yielding the following results:

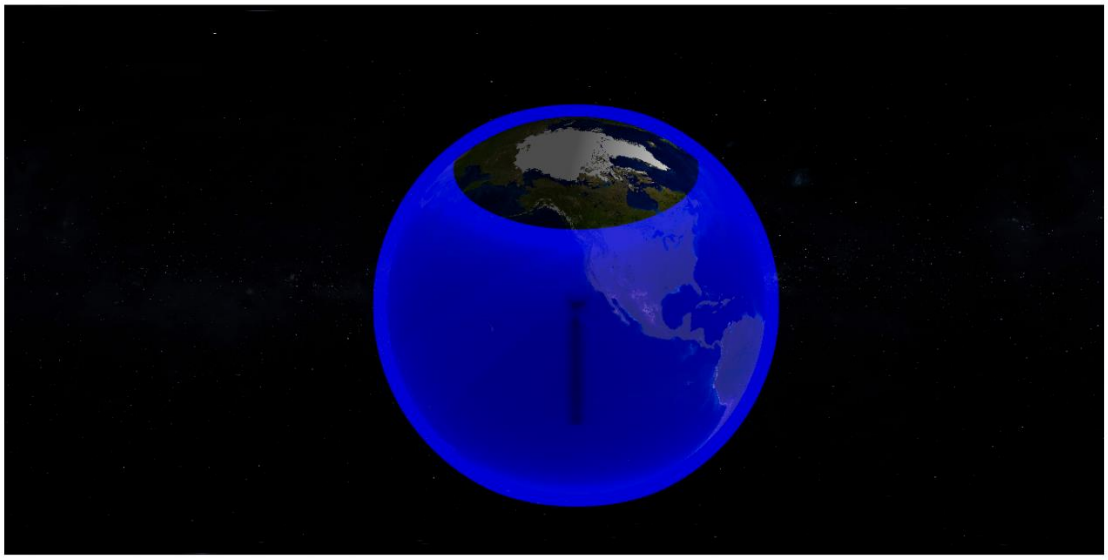

Figure 4: ECI Plot of ISS Position Over 100 days

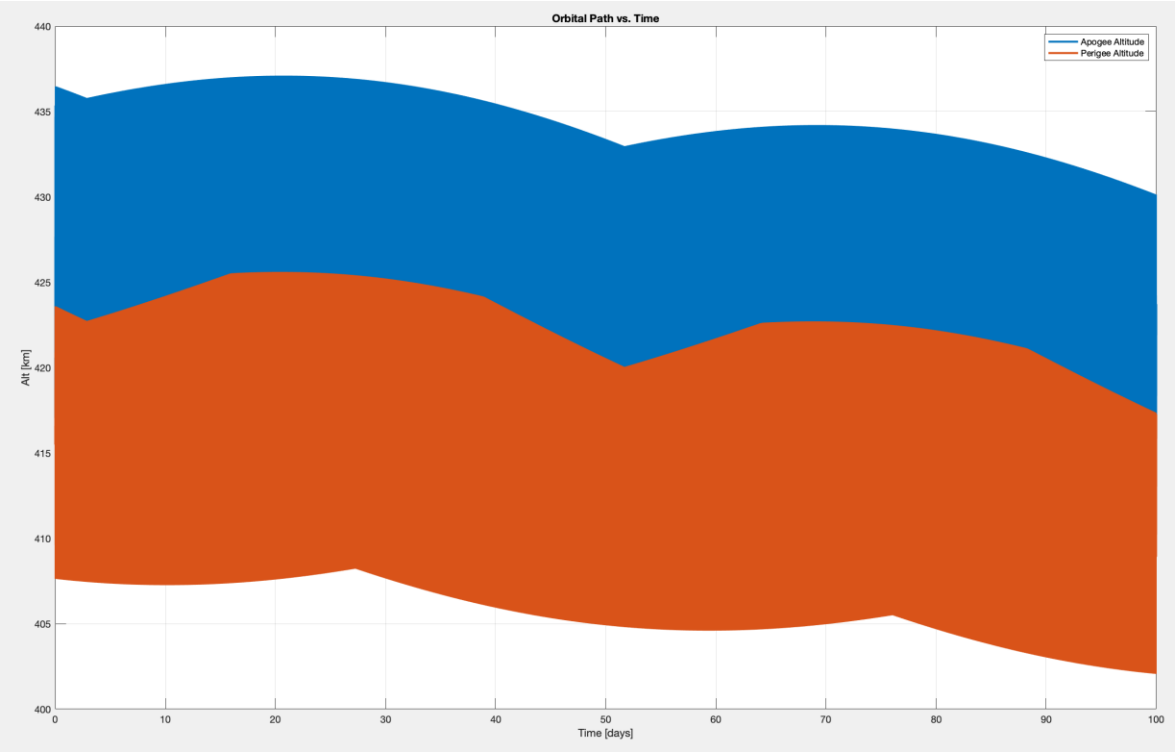

Figure 5: ISS Apogee and Perigee Altitude Over 100 days

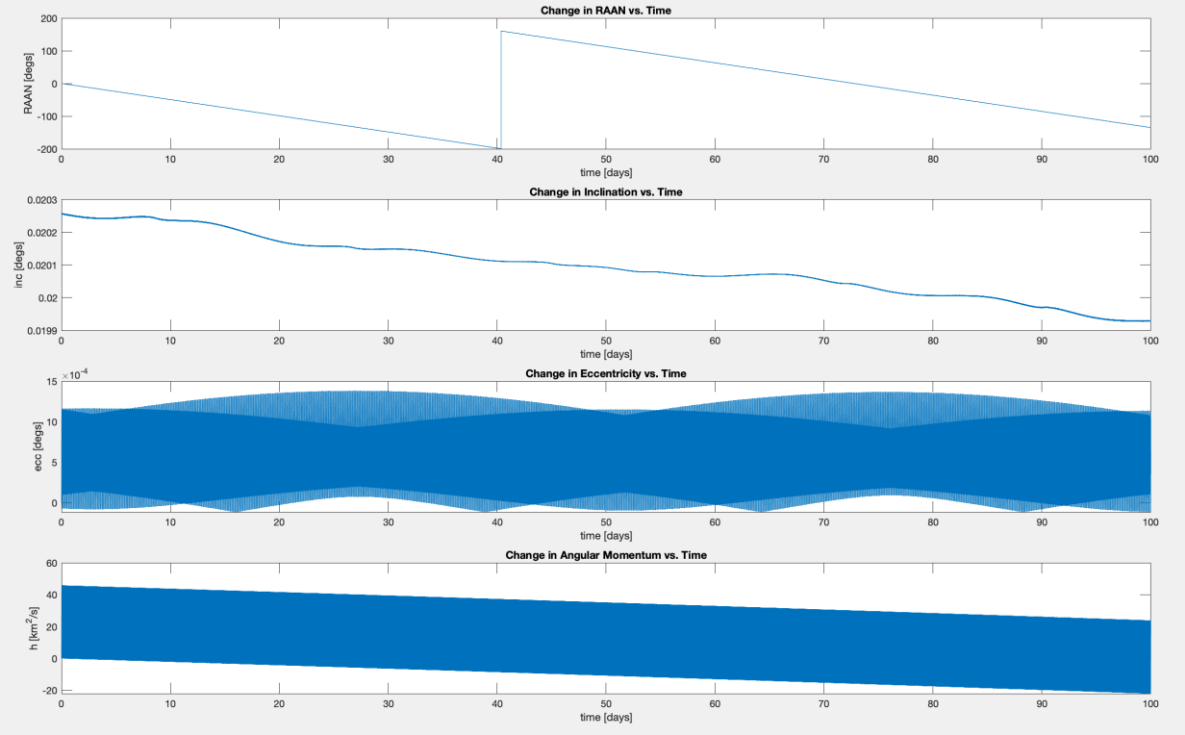

Figure 6: ISS COEs over 100 Days

Over the 100-day time span the altitudes of the apogee and perigee points can be seen to drop about 5 km. The thickness of the plot can be attributed to the length of time span compared to the orbital period of the ISS, as well as the overlap between the apogee and perigee. The drop in altitude can be almost entirely attributed to the aerodynamic drag that it experiences, with the magnitude of the solar radiation pressure being negligible in this altitude regime. This trend can also be seen in the angular momentum, which drops by about 20 $\frac{km^2}{s}$ in 100 days. There is also a very slight decrease in the inclination, which, given a standard plot over the 100 days is negligible, so instead the moving average of the inclination was plotted instead. The RAAN can be seen processing at about 5 degrees every day, due to the J2-J6 perturbation. Eccentricity remains mostly constant with slight oscillations due to the constant change in apogee and perigee radii brought about from the aerodynamic drag.

Additionally, over 100 days it is difficult to observe the periodic nature of these orbital elements, given that the ISS completes an orbit about the Earth about once every 90 minutes. In order to more clearly show the oscillatory behavior, the same plots were completed over a 1 day time span, as seen below.

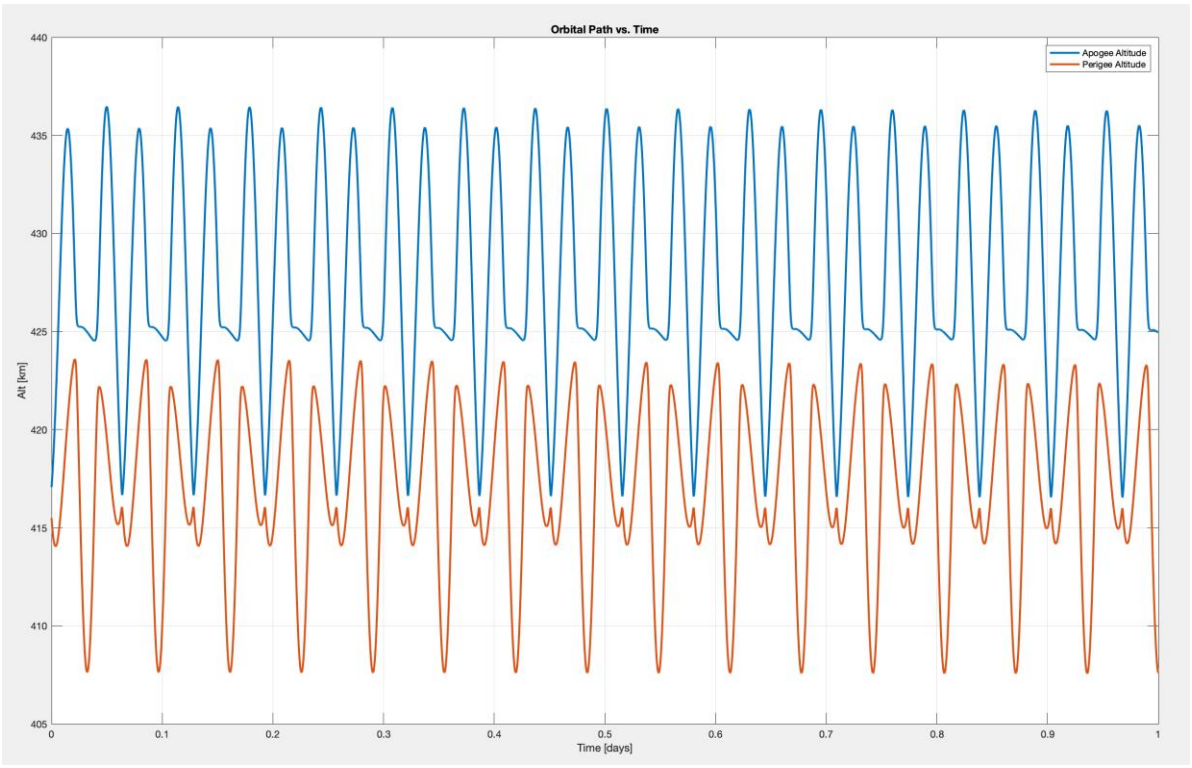

Figure 7: ISS Apogee and Perigee Altitude Over 1 day

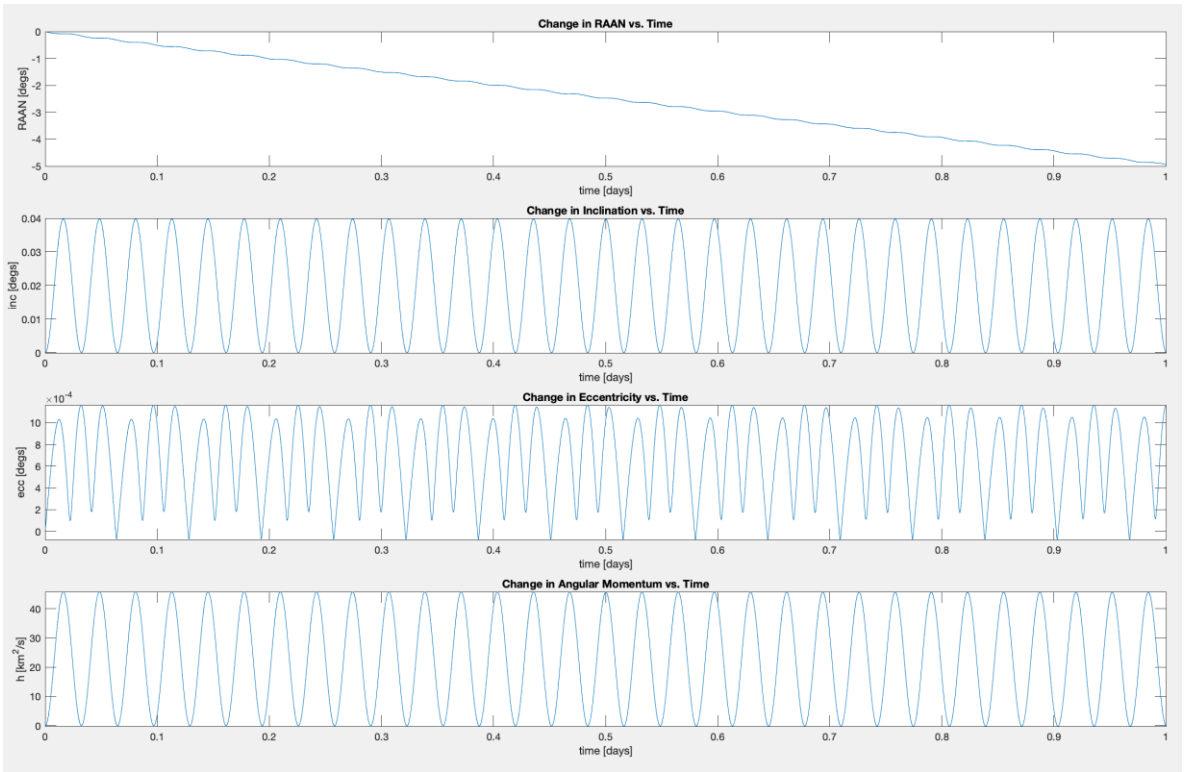

Figure 8: ISS COEs over 100 Days

An osculating orbit with no perturbations would see COEs maintain a constant line at zero, indicating no change over a 1 day period. The introduction of the J2-J6 terms as well as the n-body effects causes on oscillation of the COEs throughout the orbit. As the ISS passes the equator, the oblateness of the Earth will cause it to accelerate more, leading to the change in angular momentum and eccentricity as seen in the plots. The secular changes from drag can not be seen in these plots as they are only propagated for 1 day, leaving only the periodic behavior to be seen.

b. LEO Object Delta-V Determination and Perturbed Orbit Correction

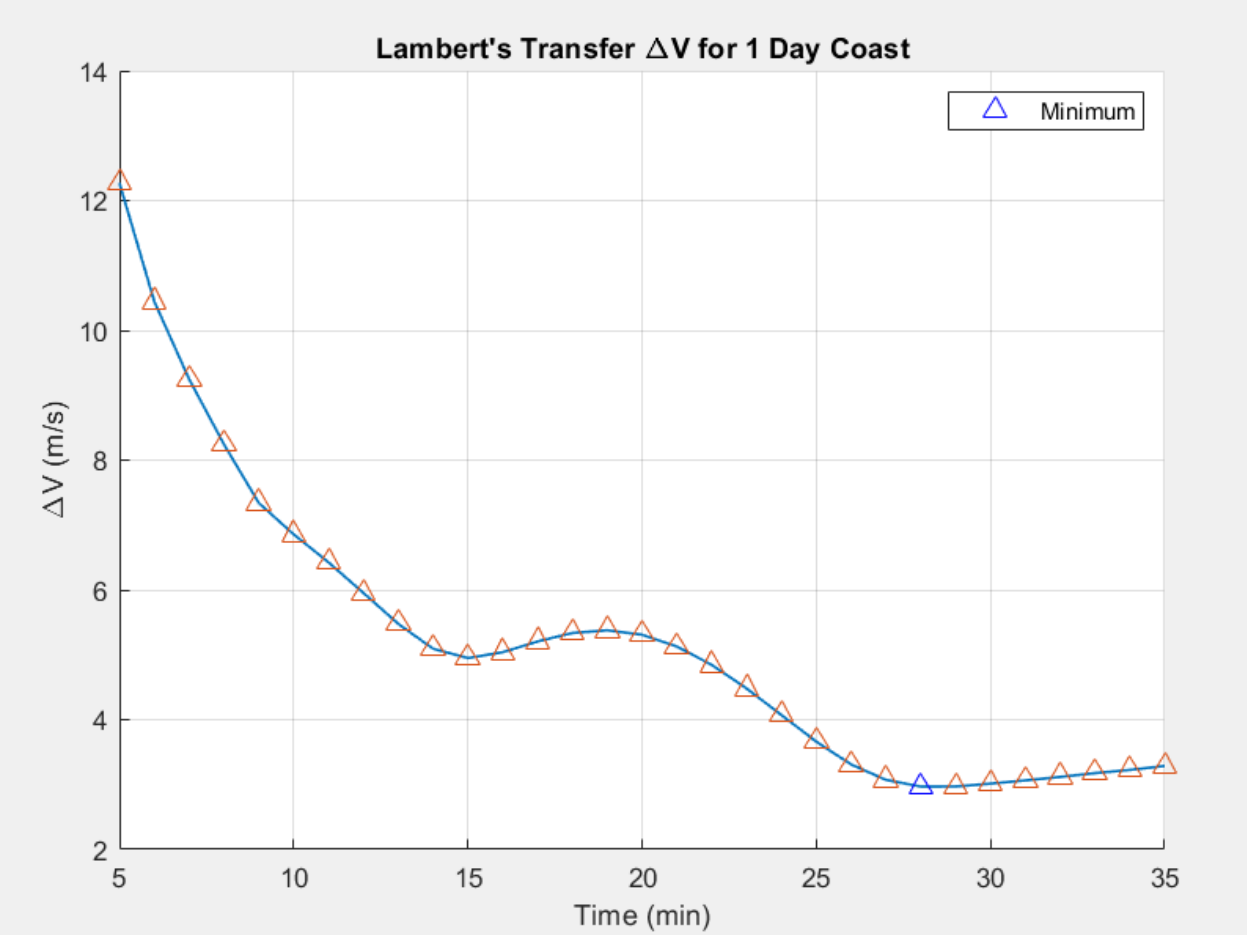

Figure 9: Delta-V optimization for 1-day drift time

In order to correct a perturbed LEO orbit, Lambert's Problem solver was used to determine a trajectory between the perturbed and osculating orbits, with the assumption that the intermediate trajectory was unperturbed. Because multiple variables influence the amount of Delta-V required to change trajectories to the intermediate, a correction frequency of 1 day is assumed, allowing for analysis and optimization of the Delta-V required for the maneuver over varying intermediate trajectory timespans.

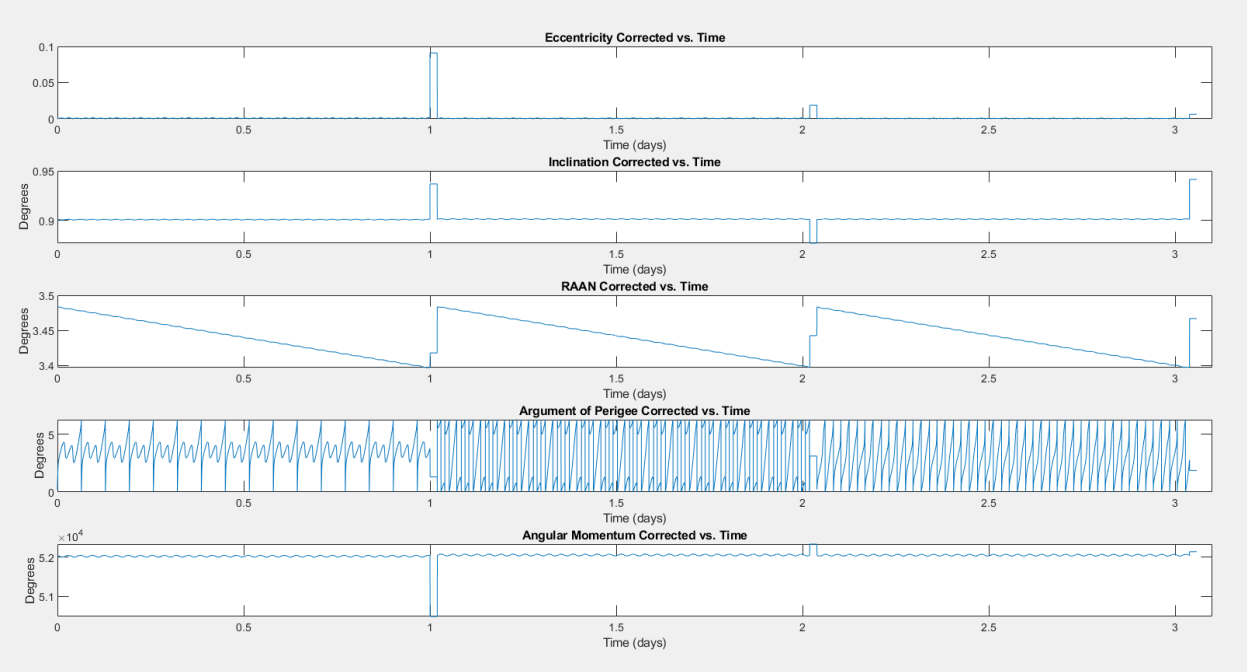

Figure 10: COEs of corrected-perturbed orbit

Seen above, the trajectory correction was applied using the optimized intermediate trajectory, requiring approximately 3 m/s per burn. While the corrected RAAN vs. time results make sense, the other elements do not exhibit the expected behavior of a progressive perturbation away from initial conditions, being reset by each corrective maneuver. Further analysis should be performed to determine the cause of this.

c. GEO Object Analysis

Next, the exact same propagation was done for the Arcturus satellite, this time neglecting aerodynamic drag due to the spacecraft operating in GEO. This yielded the following plots:

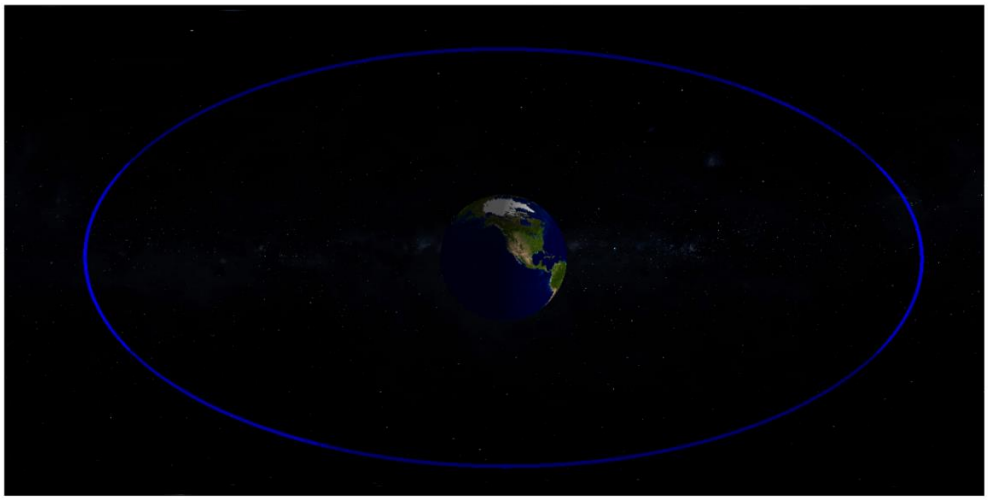

Figure 11: ECI Plot of Arcturus Position Over 100 days

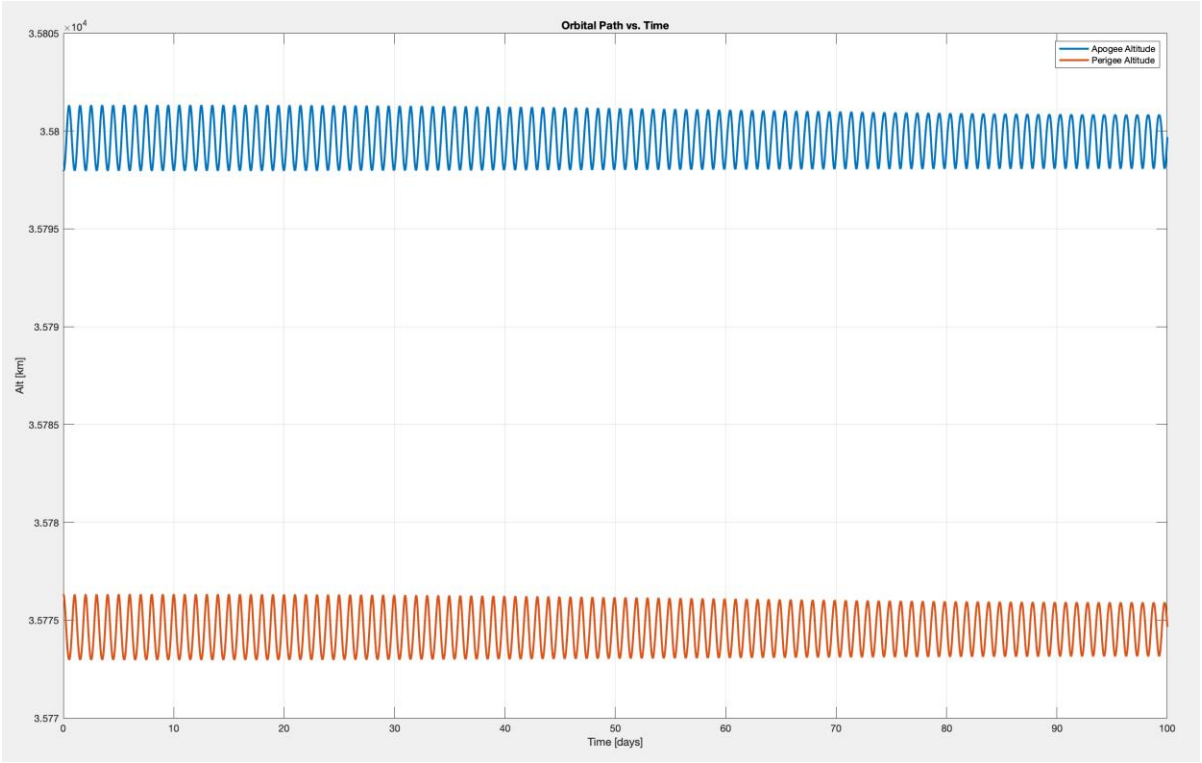

Figure 12: Arcturus Apogee and Perigee Altitude Over 1 day

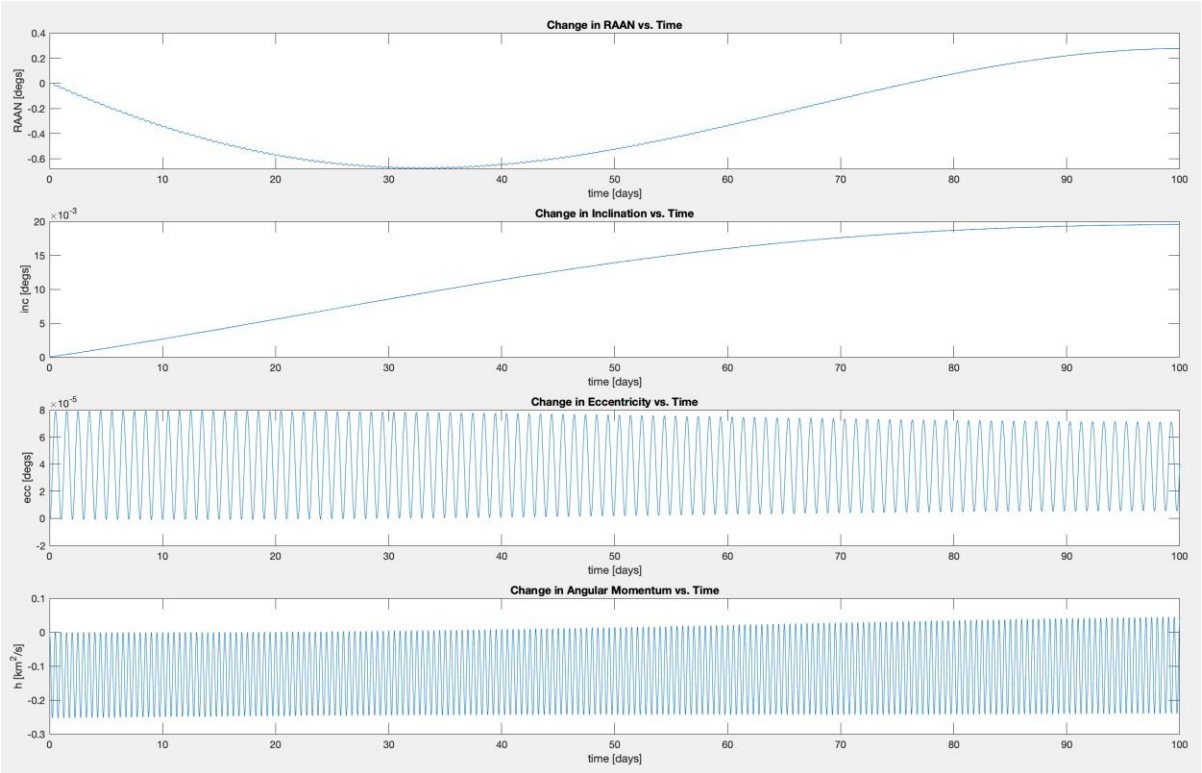

Figure 13: Arcturus COEs over 100 Days

Due to the Arcturus spacecraft operating in GEO, as well as its mass and frontal area being much less than those of the ISS, the overall perturbational forces that it experiences are far less than the ISS, due in large part to the lack of aerodynamic drag at such a high altitude. With the main non-conservative force now being SRP, it follows that the altitude will drop at a rate much lower than that of the ISS, as seen in the plots above for perigee and apogee altitudes. Also, since the object is now making a complete orbit about the Earth in about a day as opposed to every 90 minutes, the oscillations are much more visible in the 100 day propagation, this there is no need to include extra plots that propagate the object for 1 day.

The oscillations seen in the plots above can be explained by the solar radiation pressure acting on the spacecraft. As it moves through its orbit, the Sun is constantly acting on it and constantly affecting the acceleration, but essentially evens out when it reaches the opposite point in the orbit. This can be seen in the period of the oscillations, which are approximately one day.

On the plots of inclination and RAAN vs. time, long sweeping sinusoidal changes can be seen. This is again due to the effects of solar radiation pressure, but the long term effects are due to the relative motion of the Sun in the ECI coordinate frame. Evidence for this can be seen in the inclination plot, which appears to show about a quarter wavelength, meaning the full period of the oscillation is around 400 hundred days, or approximately one year.

d. Specialty Object Analysis

For Part 3, a Sun synchronous object was chosen to be studied. The Earth observation Landsat 9 satellite was chosen and propagated forward 365 days with perturbations, yielding the following ECI plot

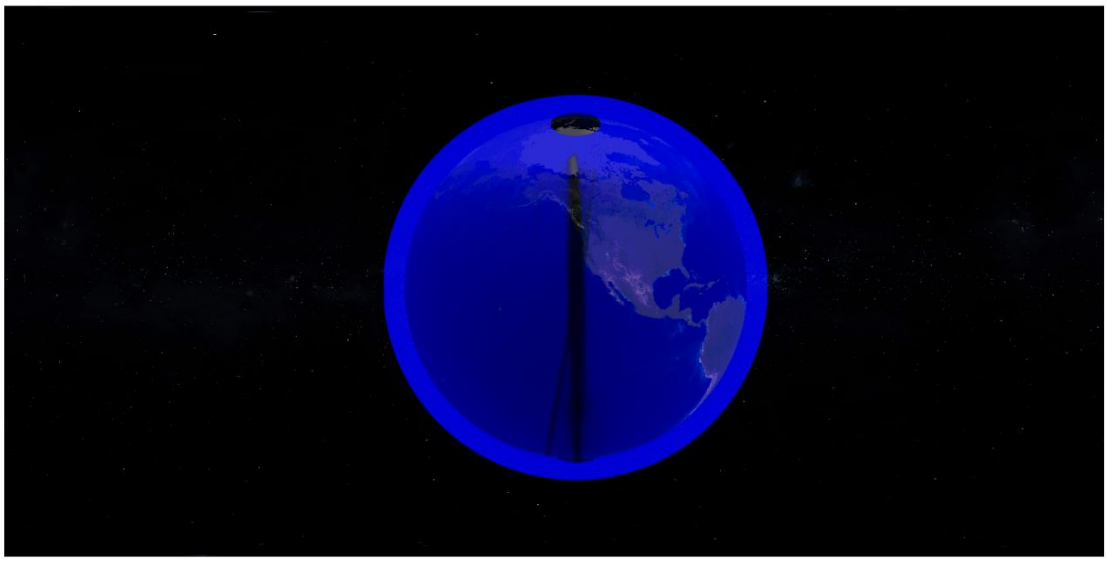

Figure 14: ECI Plot of Landsat Position Over 100 days

What makes the Sun synchronous orbit unique is its use of the J2 Earth oblateness perturbation to achieve a constant angle relative to the Sun each time it passes over a specific point on the Earth's

surface, making it optimal for Earth observation satellites like Landsat 9. Sun synchronous orbit design utilizes the nodal precession that occurs from the J2 perturbation and matches it with the rate at which the Earth rotates about the sun. As seen in Figure 11 below, the rate at which the Right Ascension of the Ascending Node processes matches perfectly with the rate at which the Earth rotates about the sun. This can be seen by the slopes of the two lines in the graph, which indicate the rate at which the RAAN and Earth rotation rate are changing. Corrections will still need to be made to account for the presence of aerodynamic drag in order to maintain sufficient altitude as well as corrections for eccentricity to maintain a circular orbit.

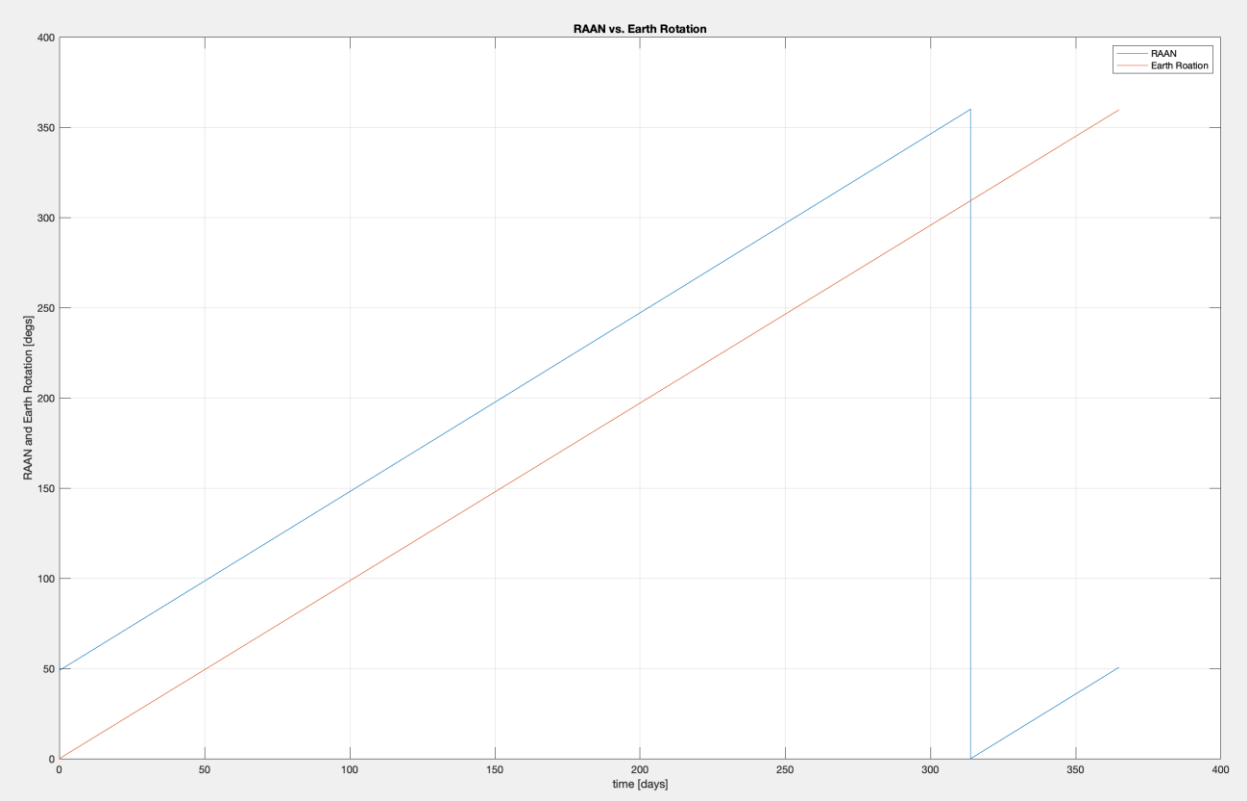

Figure 15: RAAN vs Earth Rotation for Landsat 9

IV. EXTRA ANALYSIS COMPONENT

a. Extra Component Object Analysis: Vela 8

As an extra component of this analysis, the Vela 8 spacecraft, which has extremely high apogee and perigee altitudes (approximately 160000 km and 60000 km respectively), was selected to directly examine the effect of additional bodies in the n-body perturbing acceleration, due to the fact that it's high altitudes place it nearly halfway of the altitude to the Moon at apogee. While the first body to be included in n-body acceleration is typically the Sun, the proximity of this spacecraft to the Moon made it an interesting study to examine how including both terms may affect it's orbit. Therefore, because the

purpose of this analysis was to examine the effect of additional bodies alone, it was not modeled using solar radiation pressure or atmospheric drag, so no C_d, A, or m figures are listed below.

Vela 8 was initialized with the following two-line element set (TLE):

```
1 02766U 67040B   23336.58955803 -.00001281  00000-0  00000-0 0  9991
2 02766  31.6894  23.1693 4636533  79.1908 357.5937  0.21331100  3511
```

After converting the TLE into classical orbital elements, a MATLAB function was used to compute the initial state vectors, which were propagated to visualize the osculating orbit. The results are show below:

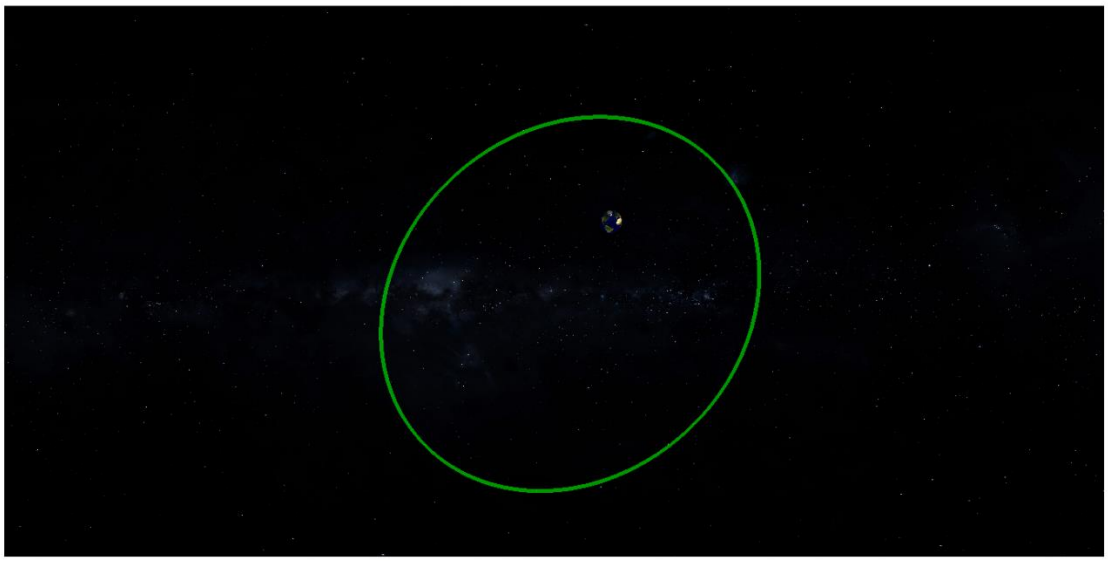

Figure 16: ECI Plot of Vela 8 osculating orbit

In order to determine the effect of additional bodies in the n-body acceleration term, Cowell's method was used to propagate the spacecraft's trajectory with solar gravitation alone perturbing the spacecraft, in addition to propagating the spacecraft's trajectory with both solar and lunar gravitational perturbations. The ECI plots of the solar-only as well as the Sun-and-Moon case are shown below:

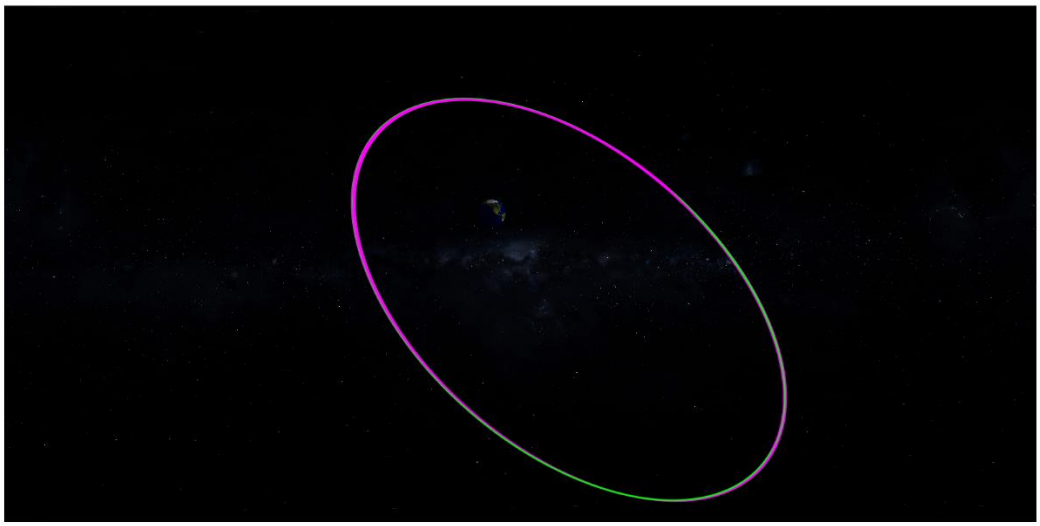

Figure 17: ECI Plot of Vela 8 perturbed orbits; Solar-only (green) and Sun-and-Moon (pink)

While it may look like a small difference between the two orbits shown in Figure 17, the scale of the orbit is actually rather large, so the small visual difference between the two shown on the plot reflects a significant difference between the two. Under closer examination, the pink trajectory (both perturbations applied) appears to sweep a wider area, while the green trajectory appears thinner. To conclude, the effects of additional bodies in the n-body perturbation is nontrivial and should be considered in cases like Vela-8 where the spacecraft has much closer approaches to additional perturbing bodies than usual.

Agreed-To-Work

As initially planned, every component of this project was created collaboratively between Mike Kabot and Kevin Iverson. All coding was performed together, and the report was written together.

Signed:

Mike Kabot

Kevin Iverson